

Mapping of few-electron wave-functions in semiconductor nanocrystals - evidence of exchange interaction

Michael Tews and Daniela Pfannkuche

I. Institute of Theoretical Physics, University of Hamburg, Jungiusstr. 9, 20355 Hamburg, Germany

Abstract. The influence of the tip-substrate bias induced electric field in a scanning-tunneling-spectroscopy experiment on charged InAs nanocrystals is studied. Calculating the ground and first excited many-particle state for five electrons occupying the quantum dot reveals a Stark-induced reordering of states by increasing the electric field strength. It is shown that this reordering of states is accompanied by a symmetry change of the local density of states (LDOS), which in principal is observable in a wave-function mapping experiment. Since in the usually performed experiments the electric field can not be directly controlled, we investigate the crystal size dependence of the 5-electron LDOS symmetry. It is found that the symmetry changes from spherical to torus-like by increasing the nanocrystal radius.

1. Introduction

Wave-function mapping in semiconductor quantum dots (QD) has recently attracted much interest since it serves as the ultimate tool to study the electronic structure of those dots [1, 2, 3]. Knowing the actual shape of the electronic densities contributes to a better understanding of the QD's electronic structure. This knowledge is crucial with respect to the possible importance of semiconductor QDs as the ultimate building blocks of optoelectronic and nanoelectronic devices.

Next to various experimental techniques available for different dot types, recent scanning-tunneling-microscopy (STM) measurements also allow an imaging of electronic densities in colloidal nanocrystals [1]. Those nanocrystals are nearly spherical in shape resulting in atomic-like symmetries and degeneracies of the electronic states [4, 5]. Nevertheless certain experiments [1] show densities with a torus-like symmetry. In the regime where electrons tunnel through neutral nanocrystals we could attribute this broken symmetry previously [6] to the electric field induced by the applied STM voltage. Although scanning-tunneling-spectroscopy (STS) experiments on colloidal nanocrystals are possible in this transport regime [7], in the usually performed experiments the nanocrystal gets charged by increasing the STM voltage. Therefore we study in this work the effect of the STM voltage on the electronic states in the regime of tunneling through already charged nanocrystals. Nevertheless the results of the earlier published single-particle calculation are also of great importance for this regime and are therefore reviewed in the first part of this paper.

We present a calculation of the many-particle conduction band (CB) states within a particle-in-a-sphere model taking into account the electric field due to the applied STM voltage. We mainly concentrate in this work on a Stark effect induced reordering of states for five electrons occupying the nanocrystal. It will be shown that this reordering corresponds to a change of the LDOS symmetry which in principal is observable in a wave-function mapping experiment.

2. Model

A sketch of the experimental setup in a STS experiment on colloidal InAs nanocrystal quantum dots is shown in Fig. 1. To obtain a tunnel spectrum the tip is positioned above a single nanocrystal attached to the substrate via hexane dithiol molecules. Keeping the tip-crystal distance constant the differential conductance as a function of applied voltage shows sharp peaks [4, 8, 9]. For a detailed understanding of the experimental data it is thus crucial to know the discrete energy spectrum of the QD since the obtained peak positions U_{peak} are directly related to the electronic dot structure [9]:

$$eU_{peak}(N, N + 1) = \gamma[E(N + 1, \alpha) - E(N, \beta)] \quad (1)$$

$$E(N, \alpha = \{n_i\}) = \sum_i n_i \epsilon_i + V_Q^{tot}(\{n_i\}) \quad (2)$$

where the pre-factor γ depends on the capacitive electrostatic geometry. For a very asymmetric tip-dot dot-substrate capacity distribution γ is close to one [9]. The total energy $E(N, \alpha = \{n_i\})$ of excitation level α with $N = \sum_i n_i$ electrons, where n_i denotes the occupation number of state i , is written as a sum of occupied single particle levels with energies ϵ_i and the total charging energy V_Q^{tot} . Hereby V_Q^{tot} includes both, the direct Coulomb interaction and all correlations.

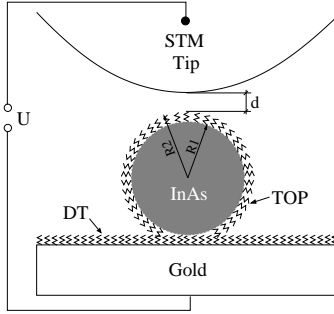


Figure 1. Scanning tunneling spectroscopy of a single InAs nanocrystal. The InAs nanocrystal with a typical radius of a few nanometers are linked to a gold substrate by hexane dithiol molecules (DT). Trioctylphosphine (TOP) molecules form a ligand shell around the nanocrystal. At 4.2K the tunnel current is measured as a function of the applied voltage U between tip and substrate.

In order to obtain the discretised energy levels (2) of the CB electrons we use a single-band envelope wave-function approximation. The confinement due to the finite crystal size is modeled by a spherical potential well with finite depth [10]. Depending on the crystal radius and the material constants of the used semiconductor those QDs can form a quite strong confinement. This confinement can lead to a size quantization of the electronic energies in the order of the semiconductor gap. Hence non-parabolicity effects of the CB have to be taken into account. Accounting for this effect we use an energy dependent effective mass approach [11] with

$$m^*(E) = m^*(0)[1 + E/E_g] \quad (3)$$

where $m^*(0)$ is the bottom CB effective mass ($0.0239 m_e$ in InAs) and E_g the bulk energy gap. This approach has proven to be quite successful in reproducing the energy gap between the single particle ground and first excited state in InAs nanocrystals [6]. In the STS setup of Fig. 1 with typical voltages up to $U \approx 2V$ [1, 4] applied on a tip-substrate distance of

a few nanometers, the QD is exposed to a considerable electric field. Therefore the model Hamiltonian for a single CB electron reads

$$H = -\frac{\hbar^2}{2m^*(E)}\nabla^2 + V_0\Theta(r - R_1) - e\Phi_e(\vec{r}) \quad (4)$$

with $\Phi_e(\vec{r})$ being the electrostatic potential. The confinement potential is described by a Heaviside function $\Theta(r - R_1)$ with the potential well depth V_0 .

The electrostatic potential $\Phi_e(\vec{r})$ is obtained from a realistic modeling of the electrostatic environment in the experimental setup of Fig. 1. While a STM tip has to terminate in a single atom in order to achieve atomic resolution, the macroscopic tip size is usually about one order in magnitude bigger than the here studied nanocrystals [12]. Other than a macroscopic metallic tip, a single terminating atom is not able to substantially focus the electric field. Over the nanocrystal size, we can therefore assume the field between tip and substrate to be homogeneous in the absence of the QD. Since these nanocrystals are typically surrounded by ligands with a quite different relative dielectric constant compared to the semiconducting crystal we model the QD as a jacketed dielectric sphere. Extending the textbook calculation of a dielectric sphere placed in a homogeneous electric field \mathcal{E}_{hom} [13] to such a structure leads to a potential inside the QD of

$$\Phi_e(r, \theta) = \frac{9\epsilon_2\mathcal{E}_{hom}r\cos\theta}{2\epsilon_2^2 + \epsilon_1\epsilon_2 + 4\epsilon_2 + 2\epsilon_1 + 2\left(\frac{R_1}{R_2}\right)^3[\epsilon_1\epsilon_2 + \epsilon_2 - \epsilon_1 - \epsilon_2^2]} \quad (5)$$

with the relative dielectric constants ϵ_1 and ϵ_2 of the nanocrystal and the ligand shell, respectively. As in the case of a dielectric sphere without a shell [13] the core potential Φ_e is still the potential of a homogeneous field. The field \mathcal{E}_{hom} occurring in (5) is not directly accessible. It is obtained by equating the voltage U with the potential drop between tip and substrate of the inhomogeneous field outside the QD. Knowing the electrostatic potential inside and also outside the nanocrystal the voltage drop over both tunneling barriers can be obtained by plotting the potential along z-direction as shown in Fig. 2. The pre-factor γ

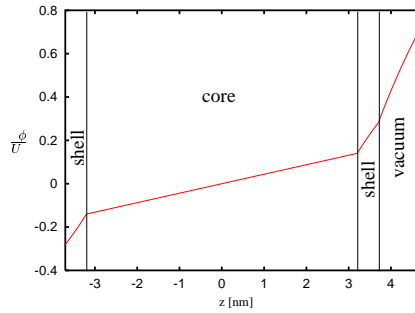


Figure 2. Electrostatic potential between STM tip and gold substrate divided by the applied tip-substrate voltage U plotted along the tip direction. The potential is calculated for an InAs nanocrystal of 3.2nm in radius and a tip-crystal distance of 1nm. The substrate is on the left and the tip starts on the very right. The dielectric constants $\epsilon_1 = 15.15$ [14] and $\epsilon_2 = 2.1$ [15] have been used for the InAs dot and the ligand shell, respectively.

of equation (1) can also be extracted from the electrostatic potential by simply relating the potential drop between tip and QD-center to the drop between QD-center and substrate.

For nanocrystals charged by N CB electrons Coulomb interaction between those electrons will be present such that the many particle Hamiltonian can be written as

$$H = -\sum_{i=1}^N \left[\frac{\hbar^2}{2m^*} \nabla_i^2 - V_0\Theta(r_i - R_1) + e\Phi_e(\vec{r}_i) \right] + \sum_{i>j}^N \frac{e^2}{4\pi\epsilon_0\epsilon_1 r_{ij}} \quad (6)$$

with ϵ_1 being the dielectric constant of the semiconducting nanocrystal. Due to the finite potential well depth the electronic wave-functions will to some extent leak out into the ligand shell. The much smaller dielectric constant in the ligand shell leads to an enhanced Coulomb interaction in this outer region compared to inside the QD. Therefore the Coulomb energy will be underestimated by this model Hamiltonian. In fact we found the charging energy for InAs nanocrystals about a factor two smaller than the experimentally observed values [4]. To account for this effect one has to replace the Coulomb operator in (6) by the proper Green's function of a dielectric sphere [16, 17]. Instead we use in this work ϵ_1 as a fitting parameter to match the experimentally found charging energy. Mirror charges induced in the metallic tip and substrate are also neglected.

3. Single-particle calculations

The single-particle Hamiltonian (4) without electrostatic potential separates in an angular and a radial part where the angular part is solved by spherical harmonics. The radial Schrödinger equation is solved by spherical Bessel functions j_l inside the well and spherical Hankel functions h_l outside [18]. The continuity conditions at the potential step lead to a set of transcendental equations determining the energy levels

$$\begin{aligned} & \alpha h_l(i\beta R_1) [l j_{l-1}(\alpha R_1) - (l+1) j_{l+1}(\alpha R_1)] \\ & = i\beta j_l(\alpha R_1) [l h_{l-1}(i\beta R_1) - (l+1) h_{l+1}(i\beta R_1)] \end{aligned} \quad (7)$$

with $\alpha = \sqrt{2m^*E}/\hbar$ and $\beta = \sqrt{2m^*(V-E)}/\hbar$. For small nanocrystals where the energy levels are in the order of the bulk energy gap the energy dependent mass of equation (3) can be directly inserted into the transcendental equation (7). Like in the hydrogen atom the single-particle ground-state has a s-type wave-function (hereafter referred to the $1S_e$ state, where the subscript e denotes an electron rather than a hole state). Other than in hydrogen the allowed orbital quantum numbers are not restricted by the principal quantum number. Hence the first excited state has the quantum numbers $n = 1$ and $l = 1$ which we will call the $1P_e$ state. Owing to the spherical harmonics, this state is threefold degenerate in the three magnetic quantum numbers $m = -1, 0$ and 1 as shown in Fig. 3a.

Knowing the single-particle states without an electric field allows now to calculate the Stark effect either by an exact diagonalization or by perturbation theory. In the case of InAs nanocrystals the results of a calculation in second order perturbation theory has proven to be sufficient [6]. Although the $1S_e$ state also shows a Stark effect, we concentrate here on the first excited $1P_e$ state. In contrast to hydrogen, the first excited state does not show a linear Stark effect, owing to the lack of s-p degeneracy in such step-like spherical potential. The $1P_e$ degeneracy is lifted by the quadratic Stark effect, such that the energy of the $1P_e(m \pm 1)$ wave-functions oriented perpendicular to the electric field are lowered compared to the $1P_e(m = 0)$ wave-function oriented along the field (see Fig. 3b).

Using the material parameters of a 3.2 nm InAs crystal leads to a Stark splitting of about 15 meV (see Fig. 3c) at an applied voltage of 1.4 V which corresponds to the experimental situation in [1]. This Stark-induced energy splitting is experimentally resolvable and allows at an appropriate voltage tunneling into the energetically lower $1P_e(m \pm 1)$ states without tunneling through the $1P_e(m = 0)$ state. The qualitatively different density distributions of those split states (see Fig. 3d), namely torus-like for the $1P_e(m \pm 1)$ and spherical for the superposition of all three p-type orbitals, are observed in a STM experiment by Millo *et al.* [1]. Therefore, the obtained Stark-induced degeneracy lifting of the first excited $1P_e$ state serves as a possible explanation for the experimentally observed mapping of the $1P_e(m \pm 1)$ wave-functions only.

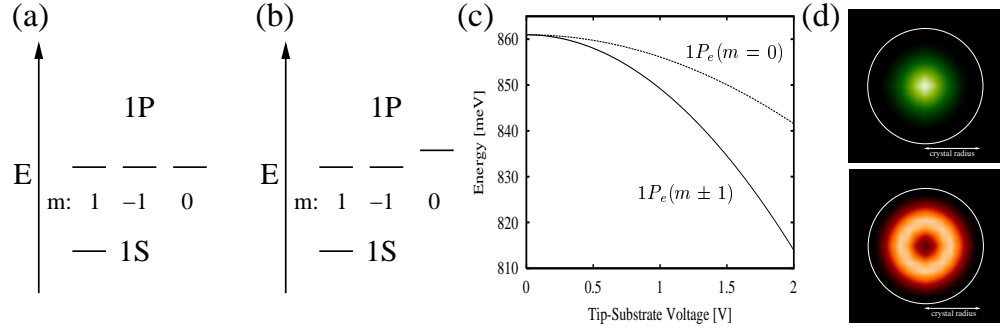


Figure 3. a) Sketch of ground and first excited state without electric field. b) Single particle energy levels with an electric field applied along z-direction. The $1P_e$ degeneracy is partly lifted. c) Stark splitting of the $1P_e$ level in a 3.2 nm radius InAs nanocrystal as a function of the applied tip-substrate voltage. For this calculation a confining potential well depth of $V_0 = 3$ eV has been used [19]. d) Electronic density of state $1P_e(m = 0)$ (top) and $1P_e(m \pm 1)$ (bottom) viewed along the applied electric field.

4. Many-particle calculation

In the usually performed experiments the p-type orbitals are available for tunneling only if the nanocrystal is already occupied by at least two electrons. Coulomb interaction between the CB electrons might be important and therefore the question arises if the single particle results of last section concerning the LDOS symmetry are still valid in this transport regime.

Solutions of the many-particle Schrödinger equation belonging to Hamiltonian (6) were found by an exact diagonalization procedure in the basis of wave-functions solving the many-particle Schrödinger equation without Coulomb interaction and without electrostatic potential. In order to keep the obtained matrices as small as possible we used the \hat{L}_z and \hat{S}_z symmetry of Hamiltonian (6) by selecting the needed basis functions. Furthermore the used basis is terminated by an energy cutoff, meaning that only Slater determinants with an energy below some threshold are used. The accuracy of a calculated energy level is estimated by the relative difference to the energy obtained by using a basis of just half the size. For all many-particle calculations presented in this work the relative error in energy is smaller than $1.5 \cdot 10^{-3}$.

4.1. Channel with 3 and 4 electrons

In the case of the first p-type channel a third electron does tunnel through the QD which is already occupied by a full $1S_e$ shell. Owing to the Stark-induced degeneracy lifting the third electron will tunnel through the energetically lower $1P_e(m \pm 1)$ state. Therefore the leading term of the 3-electron ground-state corresponds to the configuration shown in Fig. 4a. Due to the small crystal size and the high dielectric constant ($\epsilon_{InAs} = 15.15$) in those semiconducting nanocrystals the Coulomb energy is usually small compared to the kinetic energy (about 100 meV compared to 320 meV in a 3.2 nm InAs dot [4]). Therefore the LDOS will be dominated by this leading configuration and hence torus-like in symmetry.

Since the $1P_e(m \pm 1)$ states are still two-fold degenerate the fourth electron will also tunnel through one of those energetically lower states. In order to gain exchange energy both p-electrons will align their spins (Hund's rule) which is the configuration shown in Fig. 4b. The LDOS symmetry of this 4-electron ground-state will again be torus-like.

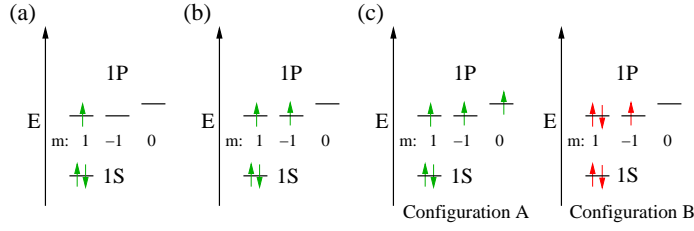


Figure 4. (a) Leading ground-state configuration for three electrons. (b) Ground-state configuration according to Hund's rule for 4 electrons occupying the nanocrystal. (c) Two possible ground-state configurations for five electrons.

4.2. Channel with 5 electrons

A more interesting situation arises for the fifth electron tunneling through the nanocrystal, where a competition between Stark energy on one hand and exchange energy on the other hand arises. Depending on how strong the splitting of the $1P_e$ states is, two different ground-states are possible. For a small splitting the configuration with all three p-type orbitals, $1P_e(m = \pm 1)$ and $1P_e(m = 0)$, occupied each by one electron with their spins aligned will be favored (see configuration A in Fig. 4c). In this configuration the fifth electron has to pay some Stark energy but gains exchange energy. On the other hand if the splitting becomes too big it is energetically more favorable for the fifth electron to occupy also a $1P_e(m \pm 1)$ state, thereby saving Stark energy. Due to the necessary spin flip however, it has to pay exchange energy (see configuration B in Fig. 4c). This competition between Stark and exchange energy leads to a ground-state crossing with increasing electric field strength (see Fig. 5). The interesting

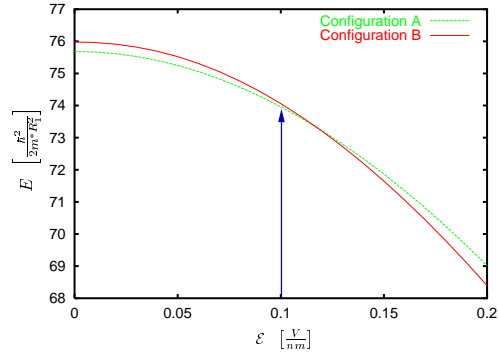


Figure 5. Ground and first excited state energies of five electrons versus the electric field strength inside a 3.2 nm radius InAs nanocrystal. The found ground-state crossing corresponds to a change in the LDOS symmetry. For this 3.2 nm dot the 5-electron channel is available at a tip-substrate voltage of about 1.5 V leading to an electric field strength indicated by the vertical arrow.

point is that this crossing also corresponds to a change in the LDOS symmetry from spherical to torus-like by increasing the electric field. In contrast to the 3- and 4-electron channel the LDOS symmetry of the 5-electron channel can be controlled by the electric field applied to the nanocrystal.

Unfortunately the electric field strength applied to the nanocrystal is determined by the corresponding peak position found in a STS experiment and, therefore, it is experimentally not straight forward to switch the LDOS symmetry forth and back between torus-like and

spherical in a wave-function mapping experiment. For a 3.2 nm InAs nanocrystal the 5-electron channel is available at a tip-substrate voltage of about 1.5 V leading to an electric field of about 0.1 V/nm. As indicated by the vertical arrow in Fig. 5 the LDOS symmetry of the ground-state is at this field strength still spherical. On the other hand the STS-peak positions depend on the QD radius such that we now stress the question how the LDOS symmetry of the 5-electron ground-state changes with the nanocrystal radius.

In order to answer the question how the ground-state symmetry depends on the crystal size the scaling behavior of the Coulomb operator versus the electrostatic potential in (6) with respect to the dot radius is studied. Whereas it is clear that the Coulomb operator scales with R_1^{-1} the scaling of the electrostatic potential is not easily foreseen. As shown in equation (5) the electrostatic potential $\Phi_e \propto \mathcal{E}_{hom}(R_1) \cdot R_1$ scales linearly with the dot radius and electric field strength. This field also depends on the dot size, but other than in a plain capacitor it scales roughly with $\mathcal{E}_{hom} \propto U(R_1) \cdot R_1^{-0.4}$. The reason for this scaling behavior is mainly the fact that the tip-crystal distance is kept constant while scaling the crystal size. Last but not least the applied tip-substrate voltage depends on the energy needed to add a further electron to the crystal which is again a function of the dot radius. In an infinite potential well the single-particle energy levels scale with R_1^{-2} but due to the finiteness of the studied potential well and the fact that the effective mass increases with increasing energy, leads to a scaling of roughly $U \propto R_1^{-1}$. Putting all together we find that the electrostatic potential scales with $\Phi_e \propto R_1^{-0.4}$. Therefore the LDOS symmetry changes from spherical to torus-like with increasing the crystal radius, since Stark energy becomes in bigger crystals more important than exchange energy.

Especially the scaling of the electrostatic potential is not straight forward and therefore it is necessary to check this result by a full calculation. To this end, the charging energy needed to add the fifth electron to the QD has to be calculated in a first step. As shown in equation (2) this charging energy is the energy difference between the 5- and 4-electron ground-states. In a second step the tip-substrate voltage needed to open this 5-electron channel has to be calculated. As shown in equation (1) this voltage is found by multiplying the charging energy with the pre-factor γ , obtained from the electrostatic potential drop along z-direction (see Section 2). Knowing the applied tip-substrate voltage, the electric field strength in the QD can in a last step be calculated by equation (5). Since the charging energy calculated in the first step also depends on the electric field, the whole cycle is repeated until self-consistency is obtained. Now knowing the electric field strength we can go back into Fig. 5 and determine the ground-state configuration for the considered QD size and therefore determine the LDOS symmetry. We have done this calculation for six InAs crystals with radii between about 2 and 6 nm and plotted the energy difference between configuration A and B versus the dot radius in Fig. 6. In this plot a number smaller than zero corresponds to a spherical and a number bigger than zero to a torus-like ground-state symmetry. As already predicted by the scaling considerations we found that the LDOS symmetry changes from spherical to torus-like by increasing the crystal radius. Using the material constants for InAs we found this transition to happen at a dot radius of about 4 nm.

5. Conclusion

We calculated the Stark effect on many-particle wave-functions in InAs nanocrystals charged with up to five electrons. Stark effect and Coulomb interactions have been fully included by an exact diagonalization procedure. We found that the LDOS, due to the Stark-induced degeneracy lifting of the $1P_e$ states, of the 3- and 4-electron ground-states are torus-like in shape. For 5 electrons however, a competition between Stark energy and exchange energy leads to a ground-state crossing with increasing field. Since the electric field strength can

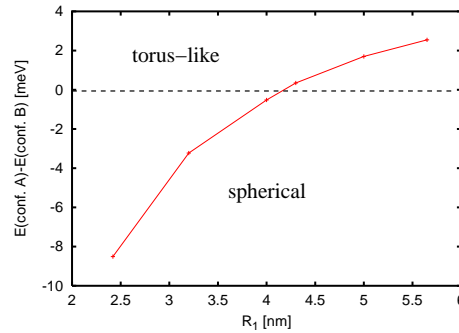


Figure 6. The difference in energy between the 5-electron ground-state and first excited state is shown as a function of nanocrystal radius. For an energy difference greater than zero, configuration B shown in Fig. 4c is the new ground-state which has a torus-like LDOS symmetry.

not be directly controlled in the usual experiments, we studied the crystal size dependence of the 5-electron ground-state symmetry and found a transition from spherical to torus-like by increasing the dot radius. This transition should be observable in a wave-function mapping experiment.

6. Acknowledgments

The authors gratefully acknowledge valuable discussions with Markus Morgenstern and Theophilos Maltezopoulos. This work was supported by the DFG through SFB 1641 and GrK 32048.

References

- [1] O. Millo, D. Katz, Y. Cao, and U. Banin, *Phys. Rev. Lett.* **86**, 5751 (2001).
- [2] B. Grandidier *et al.*, *Phys. Rev. Lett.* **85**, 1068 (2000).
- [3] E. E. Vdovin *et al.*, *Science* **290**, 122 (2000).
- [4] U. Banin, Y. Cao, D. Katz, and O. Millo, *Letters to Nature* **400**, 542 (1999).
- [5] B. Alperson *et al.*, *Applied Physics Letters* **75**, 1751 (1999).
- [6] M. Tews and D. Pfannkuche, *Phys. Rev. B.* **65**, 073307 (2002).
- [7] D. Katz, O. Millo, S.-H. Kan, and U. Banin, *Applied Physics Letters* **79**, 117 (2001).
- [8] O. Millo, D. Katz, Y. Cao, and U. Banin, *Phys. Rev. B.* **61**, 16773 (2000).
- [9] E. P. Backers and D. Vanmaekelbergh, *Phys. Rev. B.* **62**, 7743 (2000).
- [10] L. Brus, *Journal of Chemical Physics* **80**, 4403 (1984).
- [11] M. G. Burt, *J. Phys.: Condens. Matter* **4**, 6651 (1992).
- [12] R. Wiesendanger, *Scanning Probe Microscopy and Spectroscopy*, 1 ed. (Cambridge University Press, Cambridge, 1994).
- [13] D. J. Griffiths, *Introduction to Electrodynamics* (Prentice, Hall, 1998).
- [14] O. Madelung, *Semiconductors-Basic Data*, 2nd revised ed. (Springer, Berlin, 1996).
- [15] B. S. Kim, M. A. Islam, L. E. Brus, and I. P. Herman, *Journal of Applied Physics* **89**, 8127 (2001).
- [16] G. Goldoni *et al.*, *Physica E* **6**, 482 (2000).
- [17] L. D. Hallam, J. Weis, and P. Maksym, *Phys. Rev. B.* **53**, 1452 (1996).
- [18] L. I. Schiff, *Quantum Mechanics* (Springer, Berlin, 1993).
- [19] A. J. Williamson and A. Zunger, *Phys. Rev. B.* **59**, 15819 (1999).